ChemComm

Reductive activation of neptunyl and plutonyl oxo species with a hydroxypyridinone chelating ligand

Journal:	*ChemComm*
Manuscript ID	CC-COM-07-2018-005626.R1
Article Type:	Communication

ChemComm

COMMUNICATION

Reductive activation of neptunyl and plutonyl oxo species with a hydroxypyridinone chelating ligand†

Received 00th January 20xx,
Accepted 00th January 20xx

DOI: 10.1039/x0xx00000x

rsc.li/chemcomm

Korey P. Carter[a], Jiwen Jian[a], Mikaela M. Pyrch[b], Tori Z. Forbes[b], Teresa M. Eaton[a,e], Rebecca J. Abergel*[a,c], Wibe A. de Jong*[d], and John K. Gibson*[a]

Oxo group activation with reduction of neptunyl(VI) and plutonyl(VI) to tetravalent hydroxo species by the hydroxypyridinone siderophore derivative 3,4,3-LI-(1,2-HOPO) was investigated in the gas-phase via electrospray ionization mass spectrometry, in solution via Raman spectroscopy, and computationally via density functional theory. Dissociation of the gas-phase tetravalent complexes resulted in actinide-hydroxo bond cleavage.

Transuranic coordination chemistry is a topic of fundamental and practical interest as both nuclear fuel reprocessing and waste storage are areas of continuing relevance within the nuclear energy arena.[1-4] Nuclear waste is generally comprised of both actinides (An, including U, Np, Pu, Am, and Cm) and fission products (including lanthanides, Cs, and Tc) in an aqueous environment.[5, 6] In aqueous solution, U primarily exists as the hexavalent, linear uranyl cation, whereas Np and Pu prefer pentavalent and tetravalent oxidation states, respectively.[7] Although the hexavalent neptunyl and plutonyl cations are accessible under appropriate conditions, they are less stable than uranyl. Nevertheless, due to their analogous structural features (i.e. very similar An=O bond distances and angles), the actinyls form a convenient periodic series for probing structure-property relationships within the early 5f block.[8, 9] As the An=O bonds of hexavalent neptunyl and plutonyl are generally more reactive than their uranyl analogues,[10, 11] activation and functionalization of the Np=O and Pu=O bonds in these units should be more accessible. However, examples of activated neptunyl and plutonyl species remain rare due to challenges in condensed phase synthesis.

Gas-phase synthesis, via electrospray ionization (ESI) and collision induced dissociation (CID), provides a convenient route to overcome synthetic limitations and access new actinyl complexes that are otherwise unobtainable, as evidenced by three, unique monoactivated UO_2^{2+} systems that were recently prepared by CID.[12-14] We previously built on these initial studies to produce the first example of double UO_2^{2+} activation, a result of chelation by the catecholamide siderophore derivative 3,4,3-LI-CAM (hereafter denoted CAM), which yielded the first formal U(VI) non-uranyl chelate.[15] Here, we extend this line of inquiry to transuranic elements with reductive oxo activation of NpO_2^{2+} and PuO_2^{2+} via gas-phase chelation by the octadentate hydroxypyridinone ligand 3,4,3-LI-(1,2-HOPO) (hereafter denoted HOPO; structure shown in Figure 1), which features the same spermine scaffold as CAM and four 1-hydroxy-pyridin-2-one (1,2-HOPO) moieties. Neptunyl and plutonyl binding with HOPO, which is known to display a high affinity for the uranyl cation both *in vitro* and *in vivo*,[16, 17] led to reductive activation of the An=O (An = Np, Pu) bonds with formation of Np(IV) and Pu(IV) bis-hydroxo complexes.

Ethanol solutions containing approximately equimolar amounts of HOPO and $(NMe_4)_2NpO_2Cl_4$ or $PuO_2(ClO_4)_2$ were subjected to ESI in negative ion mode, which yielded 1:1 gas-phase chelates with compositions $[NpO_2(HOPO-H)]^-$ and $[PuO_2(HOPO-H)]^-$. Similar experiments were performed with ^{18}O-labeled neptunyl(VI) and plutonyl(VI), $Np^{16}O^{18}O^{2+}$ and $Pu^{16}O^{18}O^{2+}$, and complexes of both labeled and non-labeled species were selected from parent ESI mass spectra for CID. CID fragmentation of the Np and Pu chelate complexes primarily occurs via loss of two water molecules comprising the actinyl oxo-groups (*i.e.* activation), with loss of only one water molecule also observed for Np (Fig. 1). The ESI results are notable as they indicate formation of $[AnO_2(HOPO-H)]^-$ chelate complexes comprising An(IV) cations as a result of

[a] *Chemical Sciences Division, Lawrence Berkeley National Laboratory, Berkeley, CA 94720, United States.*
[b] *Department of Chemistry, University of Iowa, Iowa City, IA 52242, United States.*
[c] *Department of Nuclear Engineering, University of California, Berkeley, CA 94720, United States*
[d] *Computational Research Division, Lawrence Berkeley National Laboratory, Berkeley, CA 94720, United States.*
[e] *Present address: Embry-Riddle Aeronautical University, Department of Natural Sciences, 3700 Willow Creek Road, Prescott, AZ 86301, United States.*

†Electronic Supplementary Information (ESI) available: Experimental and computational details, additional mass spectra of species, spectroscopic data from Raman experiments, UV-Vis-NIR spectra, and coordinates and energies of computed structures. See DOI: 10.1039/x0xx00000x

reduction facilitated by HOPO. These are evidently the first examples of gas-phase two-electron actinyl reduction as only one-electron reductions have been reported previously.[10, 18, 19] In addition, the observed two-electron reduction products contrast both with the gas-phase chelate formed between the uranyl cation and HOPO, where only ligand cleavage was noted upon CID, and with previous results for the uranyl cation and CAM, where the loss of a water molecule was only observed in conjunction with cleavage of a catecholamide unit from the CAM ligand.[15]

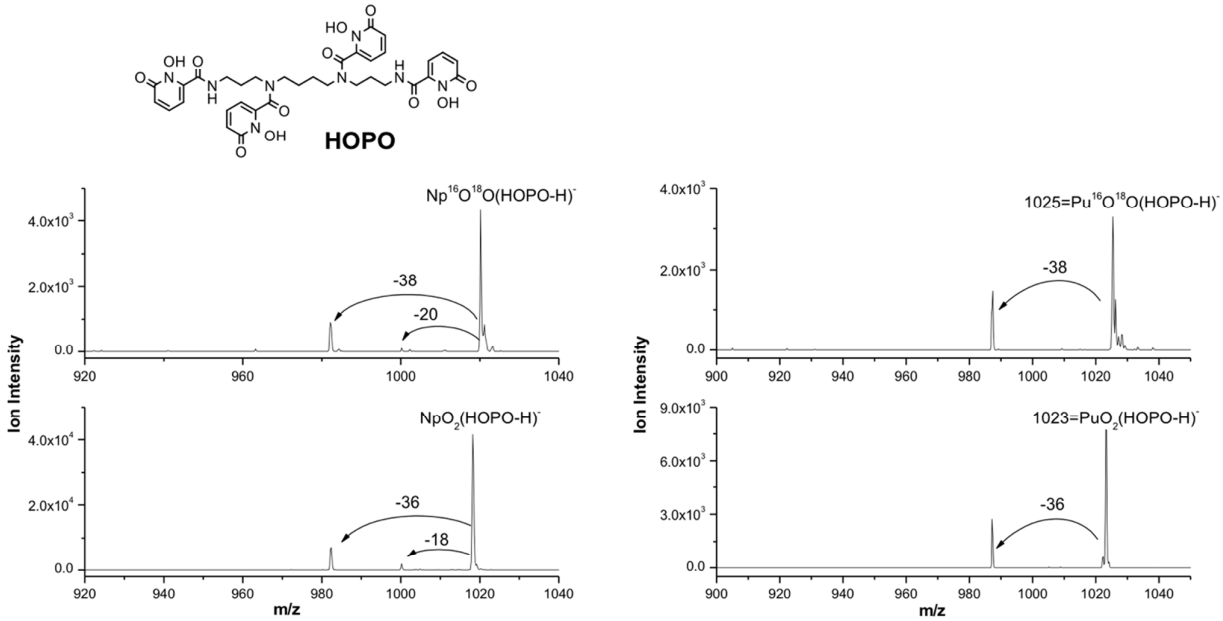

Figure 1 (Left) CID mass spectra of labeled $[Np^{16}O^{18}O(HOPO-H)]^-$ and unlabeled $[Np^{16}O_2(HOPO-H)]^-$. **(Right)** CID mass spectra of labeled $[Pu^{16}O^{18}O(HOPO-H)]^-$ and unlabeled $[Pu^{16}O_2(HOPO-H)]^-$. Nominal CID voltages=0.25 V. The dominant fragmentation pathways are losses of one or two water molecules (either $H_2{}^{16}O$ at 18 m/z or $H_2{}^{18}O$ at 20 m/z), indicating elimination of the actinyl oxo atoms during dehydration.

As CID elimination of the actinyl oxo atoms suggested that chelation with HOPO yielded Np(IV)- and Pu(IV)-dioxo species, $[NpO_2(HOPO-H)]^-$ and $[PuO_2(HOPO-H)]^-$, density functional theory (DFT) calculations were performed to gain insights into the geometrical and electronic structures. Whereas complexed dioxo species with Ce(IV) are established,[20-22] there are no known examples with tetravalent actinides, and complexed mono oxo species of Th(IV)[23, 24] and U(IV)[25-28] are also uncommon. DFT calculations found two isomers of the $[AnO_2(HOPO-H)]^-$ complexes, for both An = Np and Pu, that were close in energy, neither of which features the $An(IV)O_2$ "actinyl(IV)" moiety that was naively surmised from compositions alone. The Pu complexes are shown in Figure 2, and those with Np are analogous (Tables S1-3, ESI). The relative energies for the Np and Pu complexes, along with those of the doubly activated Np and Pu CID products (more on these below), and the calculated oxidation states, are presented in Table 1. The seven-coordinate actinide(IV) bis-hydroxide complexes, $[An(OH)_2(HOPO-3H)]^-$, (Figure 2A) were found to be the lowest energy isomers, with the oxidation states confirmed as An(IV) using Mulliken atomic spin population analysis, an approach that has been shown to provide an accurate picture of actinide oxidation states.[29, 30] Interestingly, these complexes exhibit the typical coordination environment of An(VI) cations, with the first coordination sphere of the An(IV) cations comprised of two *hydroxides*, rather than two actinyl oxo atoms, adopting *trans*-stereochemistry (An-OH bond lengths of *ca.* 2.1 Å), with five oxygen atoms from the HOPO ligand coordinating the An(IV) cations in the equatorial plane. Even though the formation of an An(IV) bis-hydroxide species from An(VI) starting materials may have been unexpected, there is precedent, especially for Np and Pu where disproportionation reactions of An(V) are known to yield An(IV) hydroxide species[31-34] similar to that highlighted in Figure 2A, with the redox non-innocent HOPO ligand used here capable of facilitating the initial reduction of An(VI) to An(V).[35, 36]

A second isomer, $[AnO(HOPO-3H)(H_2O)]^-$ (Figure 2B), was found to be only 35 (16) kJ/mol higher in energy than the bis-hydroxide for the Np (and Pu) species. Here, in addition to the five coordinating HOPO oxygen atoms, the An(IV) centers are bound by a mono oxo atom (at a typical actinyl-oxo bond distance) with the first coordination sphere completed by a water molecule *trans* to the mono-oxo atom and having an An-OH_2 distance of approximately 2.5 Å. This unusual water coordinating structure is found to be stable to dissociation of the water molecule, likely due to extensive hydrogen-bonding with the HOPO ligand. These actinide mono oxo complexes represent a new structural motif for Np(IV) and Pu(IV).

The double water loss CID product from the complex $[PuO_2(HOPO-H)]^-$ (i.e. $[Pu(HOPO-5H)]^-$) is shown in Figure 2C;

here we find an eight-coordinate actinide cation bound only to HOPO oxygen atoms (the structure is similar for the Np complex). In a recent study,[15] it was noted that loss of two water molecules was only observed when sufficient protons (in hydroxide moieties) were available on the coordinating CAM ligand. The Np- and Pu-(HOPO-H) species reported here are distinctive as only three hydroxyl protons were readily accessible for protonation, resulting in a fourth proton being abstracted from a carbon in the backbone of the ligand to yield a C atom radical (Blue Arrow in Figure 2C). Structures with the neighboring nitrogen as the radical are found to be about 35 kJ/mol higher in energy. This is admittedly a unique structure, made more so as the oxidation state for both Np and Pu was calculated to be An(III). This result implies the occurrence of a net three-electron reduction process, from An(VI) to An(III), during ESI followed by CID, which would be quite unusual, though it should be emphasized that CID water elimination to yield $[An(HOPO\text{-}5H)]^-$ is endothermic. Optimized structures of $[An(HOPO\text{-}5H)]^-$ featuring An(IV) cations were found to be ~65 kJ/mol higher in energy. The energy landscape of possible structures for the doubly dehydrated complex has many local minima, and a more comprehensive search is ongoing to ensure that the identified optimized structures are true global minima.

Table 1 Computed relative energies (in kJ/mol) and oxidation states (based on spin-density) for structures of $[An(OH)_2(HOPO\text{-}3H)]^-$ and $[AnO(HOPO\text{-}3H)(H_2O)]^-$, and reaction energy for $[AnO_2(HOPO\text{-}H)]^- \rightarrow [An(HOPO\text{-}5H)]^- + 2H_2O$.

	Relative / Reaction energy		Oxidation state	
Complex	Np	Pu	Np	Pu
$[An(OH)_2(HOPO\text{-}3H)]^-$	0 / 133	0 / 136	IV ($5f^3$)	IV ($5f^4$)
$[AnO(HOPO\text{-}3H)(H_2O)]^-$	35 / 98	16 / 120	IV ($5f^3$)	IV ($5f^4$)
$[An(HOPO\text{-}5H)]^-$	-	-	III ($5f^4$)	III ($5f^5$)

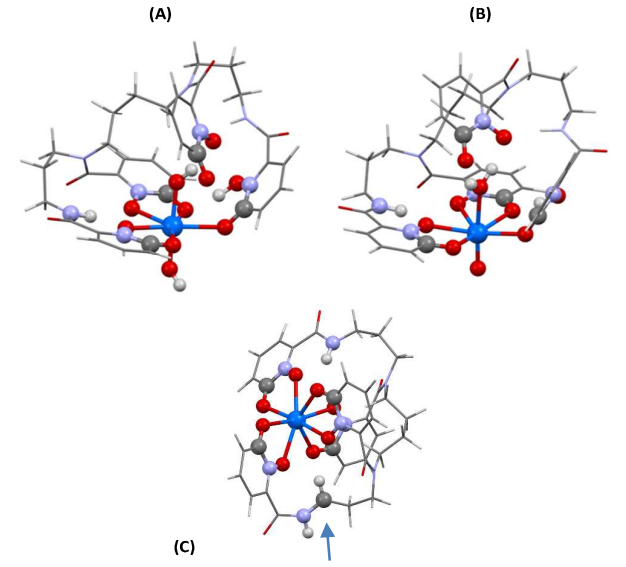

Figure 2 Computed structures of **(A)** $[Pu(OH)_2(HOPO\text{-}3H)]^-$, **(B)** $[PuO(HOPO\text{-}3H)(H_2O)]^-$, and **(C)** $[Pu(HOPO\text{-}5H)]^-$. Hydroxyl groups and other relevant atoms from the HOPO building units are highlighted in ball and stick representation. The blue arrow in **(C)** points to the carbon from which a proton has been abstracted (see text for details).

Recognizing that ESI and CID gas-phase species may not directly represent condensed phase speciation, and with the aim of improving understanding of actinyl activation, solution Raman studies were carried out on Np(V)- and Np(VI)-HOPO samples at acidic and neutral pH. A goal was to identify a potential Np(IV) mono oxo stretch, an idea inspired by a recent study by Hayton *et al*. in which Raman spectroscopy was used to confirm the formation of a terminal Ce(IV) mono oxo cation.[37] Raman spectra of the Np(V) or Np(VI) stock solution in 1 M HCl or 1 M HNO_3, respectively, were collected prior to solution state complexation with HOPO (Figure S6, ESI). The ν_1 symmetric stretching bands of Np(V) and Np(VI) in the stock solutions were located at 767 cm^{-1} and 860 cm^{-1}, respectively. Spectra of HOPO dissolved in water/methanol and buffered with HEPES/NaOH to neutral pH were also collected and no significant bands were noted in the spectral window of interest (600-900 cm^{-1}) (Figure S6, ESI).

Upon addition of the Np(V) stock to the HOPO ligand in the methanol solution, a dark grey-purple precipitate formed almost immediately (Figure S7, ESI). Raman spectra collected on the resulting colloidal solutions and the isolated powder revealed no observable bands between 600-900 cm^{-1} (Figure S8, ESI). This indicates that the ν_1 band of $Np(V)O_2^+$ is not present in the solid-state material formed upon Np-HOPO complexation. The absence of any bands in this region further suggests that there is no $Np(VI)O_2^{2+}$ or Np(IV) oxo complex in the solid. Therefore, the reaction likely occurs through a reduction of the Np(V) to an insoluble Np(IV) HOPO complex. Reduction of Np by organic chelating agents is supported by previous work of Reed *et al.*, which demonstrated reduction of Np(V) and Np(VI) to Np(IV) by citrate.[38] A thermodynamic driving force for this reduction is provided here by the very high affinity of HOPO for tetravalent metal ions.[35, 36, 39] The reaction between Np(V) and the HOPO ligand in the HEPES/NaOH buffer also resulted in a precipitate that quickly re-dissolved into the supernatant. Again, no bands were observed in the Raman spectrum of the aqueous phase (Figure S9, ESI), which may be due to higher solubility of the resulting Np(IV) complex at neutral pH.

The Np(VI)-HOPO sample also formed a dark grey-purple colloid; however, in that case the solution phase spectra also indicated residual Np(VI) after the reaction. Again, the spectrum of the resulting solid did not produce any bands within the spectral window of interest, but a small feature was noted in the solution phase. The broad band was fit using OriginPro software (Figure S10, ESI), revealing the presence of two peaks with maxima at 828 cm^{-1} (Γ = 28.26 cm^{-1}) and 808 cm^{-1} (Γ = 36.90 cm^{-1}). These band widths are within the range for previously reported aqueous phase actinyl complexes[40] and are red-shifted from the band present in the original Np(VI) stock solution. This result suggests that complexation by the

HOPO ligand occurs via two slightly different coordination environments about the $Np(VI)O_2^{2+}$ cation. The presence of residual Np(VI) in the aqueous phase indicates that the reductant was the limiting reagent in the two-electron reduction.

In summary, activation and concurrent reduction of neptunyl and plutonyl An=O bonds was achieved via ESI to yield either transuranic gas-phase An(IV) bis-hydroxo complexes, $[An(OH)_2(HOPO\text{-}3H)]^-$ (An = Np, Pu), or mono oxo isomers, $[AnO(HOPO\text{-}3H)(H_2O)]^-$, which are only slightly higher in energy. We were unable to capture either Np species in the condensed phase, yet solution state Raman spectroscopy confirmed reduction of Np(V) and Np(VI) upon complexation with HOPO, consistent with the gas-phase and computational results. CID double water elimination from the gas-phase An(IV) complexes yielded $[An(HOPO\text{-}5H)]^-$ species that feature An metal centers with oxidation states tentatively assigned as Np(III) and Pu(III). Further investigations into chelation based activation of actinyl species are in progress with both HOPO and CAM, with an emphasis on extending gas-phase results to solution and solid-state via efforts to grow single crystals of HOPO with Np(IV) and Pu(IV).

This work was supported by the U.S. Department of Energy (DOE), Office of Science, Office of Basic Energy Sciences, Chemical Sciences, Geosciences, and Biosciences Division at the Lawrence Berkeley National Laboratory under Contract DE-AC02-05CH1123 (RJA, JKG). TZF and MMP acknowledge support from DOE Heavy Elements Division (DE-SC0013980) for work associated with the Np(V) and Np(VI) reactions and Raman spectroscopy.

Conflicts of interest

The authors declare no competing financial interest.

References

1. N. Kaltsoyannis, *Chemistry – A European Journal*, 2018, **24**, 2815-2825.
2. D. D. Schnaars and R. E. Wilson, *Inorganic Chemistry*, 2018, **57**, 3008-3016.
3. G. J. P. Deblonde, M. P. Kelley, J. Su, E. R. Batista, P. Yang, C. H. Booth and R. J. Abergel, *Angewandte Chemie International Edition*, 2018, **57**, 4521-4526.
4. M. P. Kelley, G. J. P. Deblonde, J. Su, C. H. Booth, R. J. Abergel, E. R. Batista and P. Yang, *Inorganic Chemistry*, 2018, **57**, 5352-5363.
5. R. J. Silva and H. Nitsche, *Journal*, 1995, **70-71**, 377.
6. Q.-H. Hu, J.-Q. Weng and J.-S. Wang, *Journal of Environmental Radioactivity*, 2010, **101**, 426-437.
7. K. E. Knope and L. Soderholm, *Chemical Reviews*, 2013, **113**, 944-994.
8. R. G. Surbella III, L. C. Ducati, K. L. Pellegrini, B. K. McNamara, J. Autschbach, J. M. Schwantes and C. L. Cahill, *Journal of the American Chemical Society*, 2017, **139**, 10843-10855.
9. K. P. Carter, R. G. Surbella III, M. Kalaj and C. L. Cahill, *Chemistry – A European Journal*, 2018, DOI: 10.1002/chem.201801044.
10. Y. Gong, H.-S. Hu, L. Rao, J. Li and J. K. Gibson, *The Journal of Physical Chemistry A*, 2013, **117**, 10544-10550.
11. S.-X. Hu, W.-L. Li, L. Dong, J. K. Gibson and J. Li, *Dalton Transactions*, 2017, **46**, 12354-12363.
12. Y. Gong, V. Vallet, M. del Carmen Michelini, D. Rios and J. K. Gibson, *The Journal of Physical Chemistry A*, 2014, **118**, 325-330.
13. M. J. Van Stipdonk, M. d. C. Michelini, A. Plaviak, D. Martin and J. K. Gibson, *The Journal of Physical Chemistry A*, 2014, **118**, 7838-7846.
14. Y. Gong, W. A. de Jong and J. K. Gibson, *Journal of the American Chemical Society*, 2015, **137**, 5911-5915.
15. R. J. Abergel, W. A. de Jong, G. J. P. Deblonde, P. D. Dau, I. Captain, T. M. Eaton, J. Jian, M. J. van Stipdonk, J. Martens, G. Berden, J. Oomens and J. K. Gibson, *Inorganic Chemistry*, 2017, **56**, 12930-12937.
16. R. J. Abergel, P. W. Durbin, B. Kullgren, S. N. Ebbe, J. Xu, P. Y. Chang, D. I. Bunin, E. A. Blakely, K. A. Bjornstad, C. J. Rosen, D. K. Shuh and K. N. Raymond, *Health Physics*, 2010, **99**, 401-407.
17. M. Sturzbecher-Hoehne, G. J. P. Deblonde and R. J. Abergel, *ract*, 2013, **101**, 359-366.
18. D. Rios, M. C. Michelini, A. F. Lucena, J. Marçalo, T. H. Bray and J. K. Gibson, *Inorganic Chemistry*, 2012, **51**, 6603-6614.
19. P. D. Dau, D. Rios, Y. Gong, M. C. Michelini, J. Marçalo, D. K. Shuh, M. Mogannam, M. J. Van Stipdonk, T. A. Corcovilos, J. K. Martens, G. Berden, J. Oomens, B. Redlich and J. K. Gibson, *Organometallics*, 2016, **35**, 1228-1240.
20. M. P. Coles, P. B. Hitchcock, A. V. Khvostov, M. F. Lappert, Z. Li and A. V. Protchenko, *Dalton Transactions*, 2010, **39**, 6780-6788.
21. Y.-M. So and W.-H. Leung, *Coordination Chemistry Reviews*, 2017, **340**, 172-197.
22. Q. Zhu, J. Zhu and C. Zhu, *Tetrahedron Letters*, 2018, **59**, 514-520.
23. W. Ren, G. Zi, D.-C. Fang and M. D. Walter, *Journal of the American Chemical Society*, 2011, **133**, 13183-13196.
24. D. E. Smiles, G. Wu, N. Kaltsoyannis and T. W. Hayton, *Chemical Science*, 2015, **6**, 3891-3899.
25. W. J. Evans, S. A. Kozimor and J. W. Ziller, *Polyhedron*, 2004, **23**, 2689-2694.
26. G. Zi, L. Jia, E. L. Werkema, M. D. Walter, J. P. Gottfriedsen and R. A. Andersen, *Organometallics*, 2005, **24**, 4251-4264.
27. S. J. Kraft, J. Walensky, P. E. Fanwick, M. B. Hall and S. C. Bart, *Inorganic Chemistry*, 2010, **49**, 7620-7622.
28. D. E. Smiles, G. Wu and T. W. Hayton, *Journal of the American Chemical Society*, 2014, **136**, 96-99.
29. R. Maurice, E. Renault, Y. Gong, P. X. Rutkowski and J. K. Gibson, *Inorganic Chemistry*, 2015, **54**, 2367-2373.
30. J. K. Gibson, W. A. de Jong, P. D. Dau and Y. Gong, *The Journal of Physical Chemistry A*, 2017, **121**, 9156-9162.
31. R. Sjoblom and J. C. Hindman, *Journal of the American Chemical Society*, 1951, **73**, 1744-1751.
32. J. C. Sullivan, D. Cohen and J. C. Hindman, *Journal of the American Chemical Society*, 1957, **79**, 4029-4034.
33. N. K. Shastri, J. O. Wear and E. S. Amis, *Journal of Inorganic and Nuclear Chemistry*, 1962, **24**, 535-540.
34. H. Steele and R. J. Taylor, *Inorganic Chemistry*, 2007, **46**, 6311-6318.
35. G. J. P. Deblonde, M. Sturzbecher-Hoehne and R. J. Abergel, *Inorganic Chemistry*, 2013, **52**, 8805-8811.
36. G. J. P. Deblonde, M. Sturzbecher-Hoehne, P. B. Rupert, D. D. An, M.-C. Illy, C. Y. Ralston, J. Brabec, W. A. de Jong, R. K. Strong and R. J. Abergel, *Nature Chemistry*, 2017, **9**, 843-849.
37. P. L. Damon, G. Wu, N. Kaltsoyannis and T. W. Hayton, *Journal of the American Chemical Society*, 2016, **138**, 12743-12746.
38. D. T. Reed, D. G. Wygmans, S. B. Aase and J. E. Banaszak, 6th International Conference on the Chemistry and Migration Behavior of Actinides and Fission Products in the Geosphere-Migration '97, Sendai, Japan, 1997.
39. M. Sturzbecher-Hoehne, T. A. Choi and R. J. Abergel, *Inorganic Chemistry*, 2015, **54**, 3462-3468.
40. G. Lu, T. Z. Forbes and A. J. Haes, *Analytical Chemistry*, 2016, **88**, 773-780.

Table of Contents

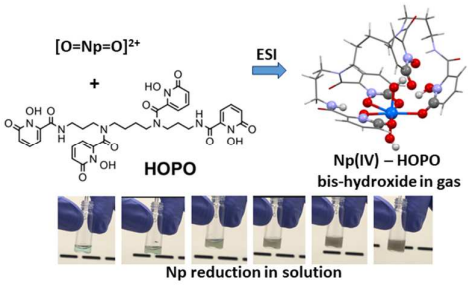

Neptunyl(VI) and plutonyl(VI) oxo-activation with reduction to tetravalent hydroxides was investigated in gas and condensed phases, and by density functional theory.

Table of Contents

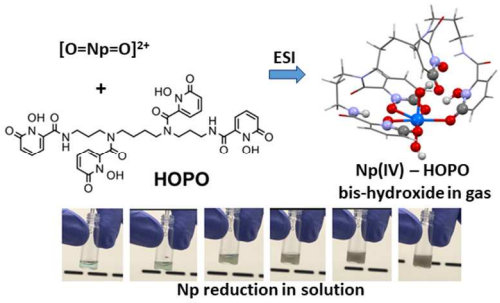

Neptunyl(VI) and plutonyl(VI) oxo-activation with reduction to tetravalent hydroxides was investigated in gas and condensed phases, and by density functional theory.